The experimental and theoretical densities in the $S_4N_3^+$ ring are in good qualitative agreement except in the N(2) and N(3) lone-pair regions. Difference maps made perpendicular to the $S_4N_3^+$ ring and passing through N(2) and N(3) show some density in the lone-pair regions, but only N(1) exhibits a clear lone-pair peak. It is doubtful that the absence of lone-pair density on N(2) and N(3) is a function of the finite data size, particularly in view of the lone-pair density observed on N(1), though it could be related to the quality of the data set which is somewhat below the optimum that can be achieved. An alternative explanation for the disagreement may be that in such a large system containing second- and third-row atoms a very extended basis set is required to achieve convergence of the theoretical density.

Acknowledgment. The authors thank the donors of the Petroleum Research Fund, administered by the American Chemical Society, for support of this work. It is also a pleasure to acknowledge stimulating discussions with Dr. E. D. Stevens of this laboratory.

Registry No. $S_4N_3NO_3$, 12033-50-0.

Supplementary Material Available: A listing of observed and calculated structure factor amplitudes (24 pages). Ordering information is given on any current masthead page.

Contribution from the Laboratoire de Chimie de Coordination du CNRS, Associé à l'Université Paul Sabatier, F-31030 Toulouse, France

Reaction of Monodentate (Tertiary phosphine)nickel(II) Complexes $NiX_2(PR_3)_2$, $NiX_2(PMe_3)_3$, and $(NiX(PMe_3)_4)(BF_4)$ with Carbon Monoxide. Crystal and Molecular Structure of $NiI_2(CO)(PMe_3)_2$

CHRISTINE SAINT-JOLY, ALAIN MARI, ALAIN GLEIZES, MICHÈLE DARTIGUENAVE,* YVES DARTIGUENAVE, and JEAN GALY

Received April 24, 1979

Nickel(II) carbonyl complexes with the general formula $NiX_2(CO)(PR_3)_2$ and $[NiX(CO)(PMe_3)_3](BF_4)$ (X = halides; PR_3 = PMe_3, PEt_3, PMe_2Ph, $PMePh_2$, PPh_3) have been obtained either by addition of carbon monoxide on the tetracoordinate $NiX_2(PR_3)_2$ compounds or by substitution of a PMe_3 ligand in the pentacoordinate $NiX_2(PMe_3)_3$ and $[NiX(PMe_3)_4](BF_4)$ complexes, in normal conditions of temperature and pressure. The structure of $NiI_2(CO)(PMe_3)_2$ was determined from the three-dimensional X-ray data. Full-matrix least-squares refinement of the structure has led to a final conventional R factor on F of 0.027. The crystals have orthorhombic symmetry, space group *Pnma*, with four molecules per unit cell of dimensions a = 10.495 (1) Å, b = 10.744 (1) Å, and c = 14.047 (2) Å. The crystal structure consists of well-separated monomeric $NiI_2(CO)(PMe_3)_2$ molecules. The geometry around the Ni atom is trigonal bipyramidal. The two trimethylphosphine groups are in axial positions. The carbonyl ligand and the two iodine atoms are located in the equatorial plane. The Ni–C bond length of 1.728 (23) Å is the shortest reported Ni–CO distance. Solid-state and solution spectroscopic determinations (UV–visible, IR, $^{31}P(^1H)$ NMR) allow the characterization of all the carbonyl complexes as trigonal bipyramids of C_{2v} symmetry for $NiX_2(CO)(PR_3)_2$ and C_s for $[NiX(CO)(PMe_3)_3](BF_4)$, CO and X being located in the equatorial plane of the bipyramid. These complexes may be easily related to the probable intermediate in the formation of acylnickel(II) complexes, in carbonylation reactions. The solvent influence is discussed.

Introduction

Although numerous examples of insertion of carbon monoxide into transition-metal carbon bonds have been reported, such examples are rare in nickel(II) chemistry.[2] It is only recently that the first acylnickel(II) complexes have been synthesized: the square-planar tetracoordinate $NiX(COCH_3)(PMe_3)_2$ (X = Cl, Br, I)[3] and the pentacoordinate $[Ni(COR)np_3]^+$ (R = CH_3, C_2H_5, $CH_3C_6H_4$; np_3 = tris(2-(diphenylphosphino)ethyl)amine).[4] This is related to the easy reduction of Ni(II) complexes by CO, giving rise to Ni(0) species.

However, in a recent work on the carbonylation mechanism with d^8 nickel, palladium, and platinum phosphine complexes, it was reported that a probable mechanism for the carbonylation reaction was a pathway through a pentacoordinate d^8 intermediate, the first-step product being shown in reaction 1.[5] Such pentacoordinate carbonyl complexes have been isolated for M = Pt(II), and the authors suggested an identical mechanism for Ni(II) complexes.

$$MXR(PR_3)_2 + CO \rightleftharpoons MXR(CO)(PR_3)_2 \qquad (1)$$

The best way to test the validity of reaction 1 for Ni(II) complexes is to study the action of carbon monoxide with Ni(II) complexes in the absence of the alkyl ligand. Thus we have studied the action of carbon monoxide on the tetracoordinate $NiX_2(PR_3)_2$ and pentacoordinate $NiX_2(PMe_3)_3$ and $(NiX(PMe_3)_4)(BF_4)$ (X = halide; PR_3 = PMe_3, PEt_3, PMe_2Ph, $PMePh_2$, PPh_3). Prior to our work, only Ni(0) complexes have been obtained when CO was allowed to react with $NiX_2(PPh_3)_2$ and $NiX_2(PEt_3)_2$.[6,7] However, to our knowledge, three exceptions were reported: $NiI_2(CO)(PMe_3)_2$,[8] $NiI_2(CO)$(fdma) (fdma = 1,1′-bis(dimethylarsino)ferrocene,[9] and the cationic $(C_6Cl_5Ni(PR_3)_2(CO))(ClO_4)$.[10]

We report here the obtainment and characterization by the usual spectrochemical techniques, for all the nickel(II) complexes, of the corresponding pentacoordinate carbonyl com-

(1) (a) Based on the Ingenieur-Docteur Thesis of C.S.J., Université Paul Sabatier Toulouse, 1978. (b) *Adv. Chem. Ser.* **1979**, *No. 173*, 152.
(2) Jolly, P. W.; Wilke, G. "The Organic Chemistry of Nickel"; Academic Press: New York, 1974; Vol. 1.
(3) Klein, H. F.; Karsch, H. H. *Chem. Ber.* **1976**, *109*, 2524.
(4) Stoppioni, P.; Dapporto, P.; Sacconi, L. *Inorg. Chem.* **1978**, *17*, 718.
(5) Garrou, P. E.; Heck, R. F. *J. Am. Chem. Soc.* **1976**, *98*, 4115.
(6) Yamamoto, K. *Bull. Soc. Chem. Jpn.* **1954**, *27*, 516.
(7) Booth, G.; Chatt, J. *J. Chem. Soc. A* **1962**, 2099.
(8) Pankowski, M.; Bigorgne, M. *J. Organomet. Chem.* **1972**, *35*, 397.
(9) Bishop, J. J.; Davison, A. *Inorg. Chem.* **1971**, *10*, 832. Pierpont, G. G.; Eisenberg, R. *Ibid.* **1972**, *11*, 828.
(10) Wada, M.; Oguro, K. *Inorg. Chem.* **1976**, *15*, 2346.

0020-1669/80/1319-2403$01.00/0

pound with the formulas $NiX_2(CO)(PR_3)_2$ and $(NiX(CO)(PMe_3)_3)(BF_4)$. A complete X-ray structural analysis has been carried out on the most stable complex, $NiI_2(CO)(PMe_3)_2$.

Experimental Section

The solvents were dried by standard methods. All the reactions were performed under an argon or a carbon monoxide atmosphere. The Ni(II) complexes $NiX_2(PR_3)_2$, $NiX_2(PMe_3)_3$, and $(NiX(PMe_3)_4)(BF_4)$ were prepared by previously reported methods.[11]

Synthesis of the Complexes. The syntheses were carried out under oxygen-free carbon monoxide. All the solvents were first deoxygenated and then saturated with carbon monoxide.

Molecular Complexes $NiX_2(CO)(PR_3)_2$ (X = Cl, Br, I; PR_3 = PMe_3, PEt_3, PMe_2Ph). $NiI_2(CO)(PMe_3)_2$: $NiI_2(PMe_3)_3$ (1 g, 1.85 mmol) was placed in a 50-mL flask fitted with a magnetic stirring bar and was dissolved in a mixture of dichloromethane and ethanol (15 mL/15 mL) at 20 °C to give a dark green solution. CO was then bubbled through the solution (which becomes red-brown and then violet) for 2 h, so as to concentrate the solution. This initiated the precipitation of brown crystals of $NiI_2(CO)(PMe_3)_2$, insoluble in ethanol. The solution was then cooled at −30 °C for 12 h. The crystals were filtered, dried under CO, and kept under CO (yield 75%). All the complexes, with the exception of $NiBr_2(CO)(PEt_3)_2$, can be handled in air for a short time.

Molecular Complexes $NiX_2(CO)(PR_3)_2$ (X = Br, I; PR_3 = $PMePh_2$, PPh_3). The same experimental procedure was employed, the only exception being the use of pure CH_2Cl_2 as solvent. Precipitation of the complexes was initiated by evaporating CH_2Cl_2 (by bubbling CO) to such an extent that cooling the solution at −30 °C for 12 h gave the crystalline compound (yield 70%).

Cationic Complexes $(NiX(CO)(PMe_3)_3)(BF_4)$ (X = Cl, Br). $(NiX(PMe_3)_4)(BF_4)$ (1.5 g, 3 mmol) was dissolved in CH_2Cl_2 (20 mL)/C_6H_6 (20 mL) at 20 °C. CO was bubbled through the solution for 1 h, and 30 mL of pentane was added. A violet-brown precipitate formed readily which was characterized as a mixture of $(NiX(PMe_3)_4)(BF_4)$ and $(NiX(CO)(PMe_3)_3)(BF_4)$. After being filtered, this product was dissolved in CH_2Cl_2 (30 mL). Bubbling CO gave an orange solution, which after concentration and cooling at −30 °C precipitated orange needles. These crystals were unstable. Only when X = Br was the complex stable enough to be handled at 20 °C under CO. In the absence of CO, it decomposed very quickly.

Physical Measurements. Magnetic, conductometric, and spectrometric (UV–visible, IR) measurements were carried out by using already described methods.[11] Phosphorus magnetic resonance spectra were recorded with a Bruker HX-90 spectrometer, calibrated with the internal-lock technique on deuterium. The solutions were prepared under argon with CH_2Cl_2/CD_2Cl_2 (1/1) or CD_2Cl_2/CF_2ClH (1/1) mixtures, $P(OMe)_3$ acting as internal reference.

X-ray Data Collection. A single crystal suitable for X-ray analysis was sealed into a Lindemann glass capillary. Preliminary precession photographs indicated Laue symmetry *mmm* and systematic absences $0kl$, $k + l = 2n + 1$, and $hk0$, $h = 2n + 1$. This is consistent with space group *Pnma* or $Pn2_1a$. Then the crystal was monted on an Enraf-Nonius CAD4 computer-controlled diffractometer. The unit cell constants were derived from a least-squares refinement of the setting angles of 25 reflections. Reflections with positive or null indices were collected up to a Bragg angle $\theta = 35°$ by using graphite-monochromatized Mo Kα radiation. Physical and crystallographic data along with data collection conditions are listed in Table I. Peak counts were corrected for background to yield net intensities I which were assigned standard deviations calculated with a conventional p factor selected as 0.02. Intensities were corrected for Lorentz and polarization effects but not for absorption since the crystal had a nearly isotropical shape with a $\mu\bar{R}$ coefficient of 0.44. A total of 709 independent reflections had $I \geq 3\sigma(I)$ and were used to refine the structure parameters.

Refinement and Structure Solution. Refinement of the structure was effected by full-matrix least-squares techniques.[12] The function minimized was $\sum w(|F_o| - |F_c|)^2$, where $|F_o|$ and $|F_c|$ are the observed and calculated structure amplitudes and the weight w is $4F_o^2/\sigma^2(F_o^2)$. The atomic scattering factors for all atoms and the anomalous terms for nickel, iodine, and phosphorus atoms were obtained from the tabulation in ref 13. The agreement indices R and R_w are defined as

$$R = \sum(||F_o| - |F_c||)/\sum F_o \qquad R_w = (\sum w(|F_o| - |F_c|)^2/\sum wF_o^2)^{1/2}$$

The centrosymmetric space group *Pnma* was assumed, and the validity of this choice was later confirmed by the structure refinement. A Patterson synthesis revealed the positions of the iodine atoms. The other nonhydrogen atoms could be located after two subsequent Fourier and one difference Fourier syntheses. Refinement of all nonhydrogen atoms using isotropic temperature factors resulted in $R = R_w = 0.072$. The introduction of anisotropic temperature factors led to $R = 0.032$ and $R_w = 0.039$. A secondary extinction effect was found to be weak through the refinement of Zachariasen's parameter ($R_w = 0.037$). Hydrogen atoms were located on a difference Fourier map. Their positions were idealized (C–H = 1 Å; P–C–H = 109.5°) and included but not refined, with fixed temperature factors $B = 6$ Å^2, in two subsequent and last cycles of refinement. The reliability factor dropped to $R = 0.027$ and $R_w = 0.029$ for the 709 reflections and 71 variables. In the last cycle, variable shifts were less than 8% of their standard deviations for Ni, I, and O atoms and less than 28% for C atoms (except 59% for β_{13} of the carbonyl carbon atom). The error in an observation of unit weight was 1.06 electrons. On the final difference Fourier map, the maximum remaining electron density did not exceed one-seventh of the value corresponding to a carbon atom on a Fourier map. Refined atomic parameters are listed in Table II. Values of observed and calculated structure amplitudes are given in Table III and are available as supplementary material. Derived root mean-square amplitudes of vibration for the atoms are listed in Table IV.

Table I

Physical and Crystallographic Data	
formula: $NiI_2(CO)(PMe_3)_2$	mol wt: 492.69
cryst system: orthorhombic	$V = 1584$ Å^3
$a = 10.495$ (1) Å	ρ_{exptl} not measd
$b = 10.744$ (1) Å	$\rho_x = 2.07$ g/cm^3
$c = 14.047$ (5) Å	$Z = 4$
space group *Pnma*	abs factor:
morphology:	$\mu_{Mo\ K\alpha} = 52.62$ cm^{-1}
spheroid ($\phi = 0.017$ cm)	

Data Collection
temp: 20 °C
radiation: λ(Mo Kα) = 0.710 69 Å
cryst-detector dist: 208 mm
detector window: height = 4mm, width = (1.60 + 4.90 tan θ) mm
takeoff angle: 3.1°
scan mode: θ–2θ
max Bragg angle: 35°
scan angle: $\Delta\theta = \Delta\theta_0 + B \tan\theta$; $\Delta\theta_0{}^a = 0.90°$; $B^a = 0.35$
values determining the scan speed: SIGPRE[a] = 0.450, SIGMA[a] = 0.018, VPRE[a] = 1°/min, TMAX[a] = 90 s
test rflctns: intensity $0\bar{7}3$, 004, $1\bar{2}0$, measured every 3600 s; orientation $1\bar{2}$,0,0, 0,$1\bar{4}$,0, 0,0,$1\bar{0}$, checked every 100 rflctns

[a] These parameters have been described: Mosset, A.; Bonnet, J. J.; Galy, J. *Acta Crystallogr., Sect. B* **1977**, *33*, 2639.

Results

Molecular Complexes $NiX_2(CO)(PR_3)_2$. The carbonyl derivatives $NiX_2(CO)(PR_3)_2$ (PR_3 = PMe_3, PEt_3, PMe_2Ph, $PMePh_2$, PPh_3; X = halide) are the only complexes characterized when carbon monoxide is bubbled through a benzene or dichloromethane solution of pentacoordinate $NiX_2(PMe_3)_3$ or tetracoordinate $NiX_2(PR_3)_2$ complexes, in the normal conditions of temperature and pressure. When X =

(11) Dawson, J. W.; Bryan, T. J.; Robinson, W.; Merle, A.; Dartiguenave, M.; Dartiguenave, Y.; Gray, H. B. *J. Am. Chem. Soc.* **1974**, *96*, 4428. Dartiguenave, M.; Dartiguenave, Y.; Gleizes, A.; Saint-Joly, C.; Galy, J.; Meier, P.; Merbach, A. *Inorg. Chem.* **1978**, *17*, 3503. Jensen, K. A.; Nielsen, P. H.; Pedersen, C. T. *Acta Chem. Scand.* **1963**, *17*, 1115. Hayter, R. G.; Humiec, F. S. *Inorg. Chem.* **1965**, *4*, 1703. Alyea, E. C.; Meek, D. W. *J. Am. Chem. Soc.* **1969**, *91*, 5761.

(12) In addition to local programs for the C11-Iris 80, local modifications of the following programs were employed: Germain, Main, and Woolfson's MULTAN program, Zalkin's FORDAP Fourier program, Ibers and Doedens' NUCLS least-squares program, Busing and Levy's ORFLS program, and Johnson's ORTEP II thermal plotting program.

(13) Cromer, D. T.; Waber, J. T. "International Tables for X-ray Crystallography"; Kynoch Press: Birmingham, England, 1965; Vol. IV, Table 2-2A. Cromer, D. T. *Ibid.*, Table 2.3.

Table II. Final Positional and Thermal Parameters for $NiI_2(CO)(PMe_3)_2$[a]

atom	x	y	z	β_{11}	β_{22}	β_{33}	β_{12}	β_{13}	β_{23}
Ni	0.30579 (19)	3/4	0.02639 (12)	7.13 (26)	6.28 (19)	3.19 (11)	0	0.02 (13)	0
I	0.21939 (7)	0.54873 (7)	0.10713 (5)	10.95 (8)	6.28 (6)	5.32 (4)	−0.80 (9)	0.00 (6)	0.88 (6)
P(1)	0.1409 (5)	3/4	−0.07310 (29)	8.9 (6)	7.7 (5)	3.32 (26)	0	−1.28 (29)	0
P(2)	0.4692 (4)	3/4	0.12615 (28)	7.4 (5)	8.8 (5)	4.7 (3)	0	−0.7 (3)	0
O	0.4759 (14)	3/4	−0.1331 (8)	15.9 (22)	20.0 (21)	5.4 (9)	0	4.0 (11)	0
C	0.4091 (21)	3/4	−0.0693 (14)	14.0 (3)	10.2 (24)	4.5 (13)	0	−2.2 (15)	0
C(11)	−0.0154 (16)	3/4	−0.0203 (12)	6.4 (21)	10.7 (22)	7.9 (14)	0	−1.2 (13)	0
C(21)	0.1387 (12)	0.8847 (10)	−0.1539 (7)	17.9 (19)	11.2 (14)	4.2 (7)	−0.9 (16)	−2.6 (10)	2.9 (8)
C(12)	0.4338 (15)	3/4	0.2517 (12)	10.7 (24)	10.7 (17)	4.3 (9)	0	−1.5 (13)	0
C(22)	0.5727 (11)	0.8823 (11)	0.1119 (9)	9.1 (15)	16.6 (18)	8.8 (10)	−6.4 (15)	−1.1 (11)	2.9 (12)
H(111)	−0.083	3/4	−0.072	6.0[b]					
H(112)	−0.029	0.825	0.019	6.0					
H(213)	0.057	0.885	−0.191	6.0					
H(211)	0.213	0.878	−0.201	6.0					
H(212)	0.149	0.964	−0.118	6.0					
H(121)	0.508	3/4	0.295	6.0					
H(122)	0.379	0.826	0.269	6.0					
H(223)	0.652	0.875	0.151	6.0					
H(221)	0.526	0.959	0.134	6.0					
H(222)	0.596	0.891	0.044	6.0					

[a] Estimated standard deviations in the least significant figure are given in parentheses in this and all subsequent tables. The form of the anisotropic thermal ellipsoid is $\exp(-(\beta_{11}h^2 + \beta_{22}k^2 + \beta_{33}l^2 + 2\beta_{12}hk + 2\beta_{13}hl + 2\beta_{23}kl))$. The quantities given in the table are the thermal coefficients × 10^3. [b] B_{iso} (Å^2).

Table IV. Root-Mean-Square Amplitudes of Vibration (Å) of Atoms in $NiI_2(CO)(PMe_3)_2$

atom	min	intermed	max
Ni	0.1784 (22)	0.192 (4)	0.200 (5)
I	0.1834 (11)	0.2350 (14)	0.2492 (11)
P(1)	0.170 (7)	0.212 (7)	0.232 (7)
P(2)	0.196 (7)	0.223 (8)	0.227 (8)
O	0.192 (21)	0.326 (19)	0.342 (18)
C	0.196 (30)	0.244 (29)	0.292 (32)
C(11)	0.185 (31)	0.250 (26)	0.285 (24)
C(21)	0.159 (20)	0.269 (18)	0.330 (17)
C(12)	0.192 (25)	0.251 (19)	0.256 (27)
C(22)	0.175 (23)	0.274 (18)	0.361 (18)

CN and $PR_3 = PMe_3$, no reaction is observed.

Analytical data for the different complexes are reported in Table V. They are all pentacoordinate, monomeric, molecular, and diamagnetic with a low dipole moment value. They are fairly stable in the solid state and in solution if kept under carbon monoxide. Under an inert atmosphere, they evolve CO easily, reverting to the original tetracoordinate species as demonstrated by analysis of the final complexes (reaction 2). The experimental stability order toward CO

$$NiX_2(CO)(PR_3)_2 \rightleftharpoons NiX_2(PR_3)_2 + CO \qquad (2)$$

dissociation of $NiX_2(CO)(PR_3)_2$ is I > Br > Cl, the order observed for the pentacoordinate Ni(II) complexes,[11] and $PMe_3 > PEt_3 \approx PMe_2Ph > PMePh_2 > PPh_3$, i.e., the steric hindrance of the phosphine ligand.[14] One exception is observed, i.e., $NiBr_2(CO)(PEt_3)_2$, which is very unstable. The same phosphine order has been observed in the $CoX_2(CO)(PR_3)_2$ pentacoordinate complexes, where CO dissociation has been related to phosphine size.[15]

These complexes show, in the solid state and in dichloromethane solution (Table VI), an infrared absorption in the region 2000–2040 cm^{-1} assignable to ν(CO), consistent with the existence of only one stereoisomer. There are, however, two exceptions: $NiBr_2(CO)(PMe_2Ph)_2$ and $NiBr_2(CO)(PMePh_2)_2$ for which the solid-state IR spectrum is characterized by a second CO vibration appearing as a shoulder at higher energy. Only one X-ray determination would enable us to decide if these IR spectra may be interpreted either by the presence of two stereoisomers or by a solid-state distortion. Such a problem has been observed in the nitrosyl complex $CoCl_2(NO)(PR_3)_2$.[16] From Table VI, it is apparent that, in CH_2Cl_2 solution, the decrease of ν(CO) parallels the increase of the phosphine basicity,[17] but no simple relation between the two factors can be deduced.

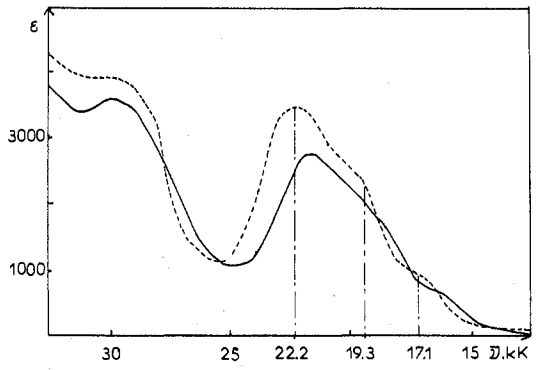

Figure 1. Temperature dependence of the electronic spectrum of $NiI_2(CO)(PMe_3)_2$ (10^{-2} M) in dichloromethane saturated with CO: —, 295 K; - - -, 190 K.

Electronic spectral data for the dichloromethane solutions are reported in Table VII. They are similar to the solid-state data. The electronic spectra of the complexes show a low-energy transition in the range 15 000–25 000 cm^{-1}, which can be resolved by Gaussian analysis into a three-band system. Lowering the temperature of the solution to 180 K increases the resolution of the spectrum as shown in Figure 1 and indicates that the same chemical species are preserved in solution between 295 and 180 K. The frequency of these three low-energy transitions is shifted in accordance with the position of the donor atoms in the spectrochemical series Cl > Br > I and $PEt_3 > PMe_3 > PMe_2Ph > PMePh_2 > PPh_3$. These spectra can be correlated to those of the corresponding trigonal-bipyramidal complexes $NiX_2(PMe_3)_3$ of C_{2v} symmetry.[1] Thus, if the same geometry is preserved for all the carbonyl complexes, the two lowest energy transitions (ϵ 500) may be assigned to the two expected ligand field transitions $A_1 \rightarrow A_1$ ($d_{x^2-y^2} \rightarrow d_{z^2}$) and $A_1 \rightarrow B_2$ ($d_{xy} \rightarrow d_{z^2}$). The third transition, more intense (ϵ in the range 2000–6000), is certainly related with CO, since such a transition is not observed in the absence of CO. But its dependence on the spectrochemical series indicates too that it is phosphine and halide dependent.

^{31}P NMR data for the different complexes are reported in Table VIII. Since nickel(II) phosphine complexes are known to be stereochemically nonrigid, low-temperature spectra (190 K) have been determined. Comparing the spectra of $NiX_2(CO)(PMe_3)_2$ and $NiX_2(PMe_3)_3$ (where an axial and equatorial PMe_3 chemical shift range (in ppm) has been determined[18]) indicates that the two phosphine

(14) Tolman, C. A. *Chem. Rev.* **1977**, *77*, 313.
(15) Bressan, M.; Corain, B.; Rigo, P.; Turco, A. *Inorg. Chem.* **1970**, *9*, 1733.
(16) Brock, C. P.; Collman, J. P.; Dolcetti, G.; Farnham, P. H.; Ibers, J. A.; Lester, J. E.; Reed, C. A. *Inorg. Chem.* **1973**, *12*, 1304.
(17) Streuli, C. A. *Anal. Chem.* **1960**, *32*, 985.
(18) Meier, P.; Merbach, A.; Dartiguenave, M.; Dartiguenave, Y. *Inorg. Chem.* **1979**, *18*, 610.

Table V. General Physical Data and Analysis of the $NiX_2(CO)(PR_3)_2$ and $[NiX(CO)(PMe_3)_3](BF_4)$ Complexes

compd	color	mol wt[b]	Λ_c[a]	μ_{eff}, μ_B	dipole moment[c]	%C calcd	%C found	%H calcd	%H found
$NiCl_2(CO)(PMe_3)_2$	red-brown	*d*	0.3[a]	0.48	3.05	27.14	26.92	5.86	5.82
$NiBr_2(CO)(PMe_3)_2$	brown	408 (399)	1.5[a]	0.47	2.76	21.09	20.78	4.55	4.65
$NiI_2(CO)(PMe_3)_2$	dark brown	463 (493)	0.2[a]	0.52	2.95	17.07	17.03	3.69	3.56
$NiBr_2(CO)(PMe_2Ph)_2$	brown	*d*	0.4[a]	0.18	3.66	39.05	39.16	4.24	4.28
$NiI_2(CO)(PMe_2Ph)_2$	red-violet	*d*	0.6[a]	0.46	2.79	33.10	33.17	3.60	3.58
$NiBr_2(CO)(PMePh_2)_2$	brown	*d*	1.2[a]	0.34	5.05	50.12	49.86	4.05	4.10
$NiI_2(CO)(PMePh_2)_2$	violet	*d*	0.5[a]	0	4.20	43.72	43.60	3.54	3.50
$NiBr_2(CO)(PPh_3)_2$	orange-brown	*d*	*d*	0.5	*d*		*e*		*e*
$NiI_2(CO)(PPh_3)_2$	violet	*d*	*d*	0.9	*d*		*e*		*e*
$NiBr_2(CO)(PEt_3)_2$	orange	*d*	*d*	*e*	3.10		*e*		*e*
$NiI_2(CO)(PEt_3)_2$	dark brown	587 (577)	1.4[a]	0	4.07	27.06	27.18	5.24	5.23
$[NiCl(CO)(PMe_3)_3](BF_4)$	orange	*d*	*d*	*e*	*f*		*e*		*e*
$[NiBr(CO)(PMe_3)_3](BF_4)$	orange	*f*	*f*	*e*	*f*	24.94	24.88	5.65	5.74

[a] Equivalent conductance of 10^{-3} M solution in nitrobenzene. [b] Molecular weight determined by cryoscopy in benzene. The theoretical values are in parentheses. [c] The dipole moment (μ) is obtained in benzene (10^{-2} M). [d] The complex is decomposed in solution. [e] Unstable. [f] Insoluble in C_6H_6.

Table VI. ν(CO) Absorptions (cm^{-1}) for the $NiX_2(CO)(PR_3)_2$ and $[NiX(CO)(PMe_3)_3](BF_4)$ Complexes

compd	CH_2Cl_2 soln	solid state[a]
$NiCl_2(CO)(PMe_3)_2$		2005
$NiBr_2(CO)(PMe_3)_2$	2018	2010
$NiI_2(CO)(PMe_3)_2$	2019	2015
$NiBr_2(CO)(PMe_2Ph)_2$	2022	2012, 2025
$NiI_2(CO)(PMe_2Ph)_2$	2023	2022
$NiBr_2(CO)(PMePh_2)_2$	2026	2015, 2030
$NiI_2(CO)(PMePh_2)_2$	2027	2018
$NiBr_2(CO)(PPh_3)_2$		decomp
$NiI_2(CO)(PPh_3)_2$		2025
$NiBr_2(CO)(PEt_3)_2$	2011	2004
$NiI_2(CO)(PEt_3)_2$	2012	2003
$[NiBr(CO)(PMe_3)_3](BF_4)$	2040	2030

[a] Nujol mull.

Table VII. Solution Electronic Spectra of the $NiX_2(CO)(PR_3)_2$ and $[NiX(CO)(PMe_3)_3]^+$ Complexes ($\bar{\nu} \times 10^{-3}$, cm^{-1} (ϵ))[a]

compd	T, K	CH_2Cl_2 soln with excess CO		
$NiCl_2(CO)(PMe_3)_2$	295	19.2 (430)	22.7 (760)	26.7 (4950)
	190	19.5 (460)	22.8 (900)	27.0 (6370)
$NiBr_2(CO)(PMe_3)_2$	295	17.9 (590)	21.9 (1500)	24.8 (4150)
	190	18.3 (1020)	22.2 (1130)	25.9 (4570)
$NiI_2(CO)(PMe_3)_2$	295	16.2 (400)	19.0 (1300)	21.8 (2400)
	190	17.1 (890)	19.3 (1130)	22.2 (3500)
$NiBr_2(CO)(PMe_2Ph)_2$	295	17.3 (270)	21.6 (1010)	24.6 (4790)
	190	17.9 (500)	21.2 (690)	24.5 (5030)
$NiI_2(CO)(PMe_2Ph)_2$	295	15.8 (590)	17.8 (730)	20.8 (2950)
	190	16.1 (650)	17.8 (1060)	21.2 (3960)
$NiBr_2(CO)(PMePh_2)_2$	295	16.5 (230)	20.9 (970)	23.5 (3900)
	190	17.3 (700)	21.1 (690)	23.5 (4300)
$NiI_2(CO)(PMePh_2)_2$	295	15.3 (420)	17.7 (690)	20.0 (2530)
	190	15.5 (580)	17.2 (1300)	20.5 (4230)
$NiBr_2(CO)(PPh_3)_2$	190	16.8 (400)	19.8 (740)	22.0 (4400)
$NiI_2(CO)(PPh_3)_2$	190	14.4 (320)	15.8 (560)	18.8 (2400)
$NiBr_2(CO)(PEt_3)_2$	295	18.1 (430)	22.3 (980)	24.9 (3900)
	190	18.9 (690)	22.9 (1650)	25.2 (3990)
$NiI_2(CO)(PEt_3)_2$	295	16.6 (465)	19.2 (1220)	21.5 (3070)
	190	17.7 (1090)	20.4 (1600)	22.2 (3430)
$[NiBr(CO)(PMe_3)_3]^+$	295	17.4 (100)	21.3 (420)	25.0 (1280)
	190	17.8 (390)	21.7 (820)	25.3 (1790)

[a] The values are not corrected from the solvent contraction between 295 and 180 K.

ligands are equivalent (a singlet) and located at the axial sites of the trigonal bipyramid. This is in agreement with the X-ray structure (vide infra). A strong downfield shift is observed (δ_{PMe_3} = 16.6 for $NiBr_2(CO)(PMe_3)_2$ compared to δ_{PMe_3ax} = −3.7 in $NiBr_2(PMe_3)_3$). The presence of only a singlet for all the $NiX_2(CO)(PR_3)_2$ complexes (Table VIII) indicates that the same trigonal-bipyramidal stereochemistry is present. This is in agreement with the dipole moment values which are in the same range (Table V). Figure 2 shows the

Table VIII. $^{31}P\{^1H\}$ NMR Data[a]

compd	δ (ligand)	δ (compound)	Δδ
$NiCl_2(CO)(PMe_3)_2$	−62	21.6	83.6
$NiBr_2(CO)(PMe_3)_2$	−62	16.6	78.6
$NiI_2(CO)(PMe_3)_2$	−62	6.6	68.6
$NiBr_2(CO)(PMe_2Ph)_2$	−46	17.7	63.7
$NiI_2(CO)(PMe_2Ph)_2$	−46	10.9	56.9
$NiBr_2(CO)(PMePh_2)_2$	−28	30.2	58.2
$NiI_2(CO)(PMePh_2)_2$	−28	24.8	52.8
$NiBr_2(CO)(PPh_3)_2$	−60	34.1	40.1
$NiI_2(CO)(PPh_3)_2$	−60	33.4	39.4
$NiBr_2(CO)(PEt_3)_2$	−20.1	40.8	60.9
$NiI_2(CO)(PEt_3)_2$	−20.1	35.1	55.2
$[NiBr(CO)(PMe_3)_3](BF_4)$	−62	$17(d_{ax}) - 26.6(t_{eq})$	

[a] $\Delta\delta = \delta$(complex) − δ(ligand); d = doublet, t = triplet; δ in ppm (positive shift downfield from 62.5% H_3PO_4); CH_2Cl_2 as solvent; at 190 K.

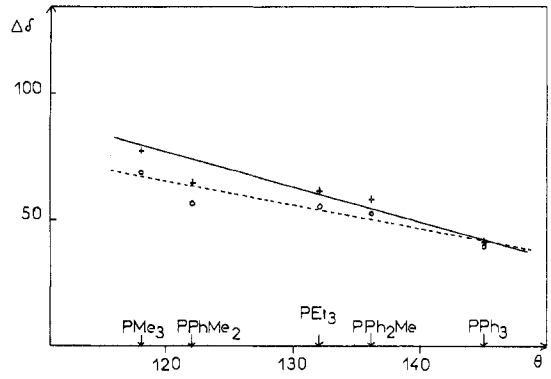

Figure 2. Correlation of chemical shift variation $\Delta\delta$ with cone angle θ in $NiX_2(CO)L_2$ complexes (X = Br, Cl) ($\Delta\delta = \delta_{^{31}P}$(complex) − $\delta_{^{31}P}$(free ligand)).

variation of the chemical shift ($\Delta\delta = \delta_P$(complex) − δ_P(free phosphine)) as a function of θ, Tollman's cone angle of the phosphine. A good correlation is observed between the two parameters, thus agreeing with an identical structure of the different complexes in solution.[14,19]

A complete X-ray structural analysis has been carried out on $NiI_2(CO)(PMe_3)_2$. The crystal structure consists of discrete, well-separated $NiI_2(CO)(PMe_3)_2$ molecules. The unit cell contains four molecular entities. The nickel atom, the carbon monoxide atoms, and two methyl group carbon atoms lie in the mirror *m* of the unit cell. The iodine atoms and the other methyl groups are symmetrically related through this mirror. Selected interatomic distances and angles are given in Table IX. The numbering scheme and a perspective view of the molecule are shown in Figure 3. The geometry around

(19) Verkade, J. G. *Coord. Chem. Rev.* **1972–1973**, *9*, 1.

Table IX. Intramolecular Main Bond and Nonbonded Distances (Å) and Angles (Deg) in $NiI_2(CO)(PMe_3)_2$

Distances around Ni			
Ni-I	2.6048 (13)	Ni-P(2)	2.215 (5)
Ni-I′	2.6048 (13)	Ni-C	1.728 (23)
Ni-P(1)	2.225 (5)		
Angles around Ni			
I-Ni-I′	112.23 (7)	I-Ni-P(2)	89.66 (8)
I-Ni-C	123.88 (4)	I′-Ni-P(2)	89.66 (8)
I′-Ni-C	123.88 (4)	C-Ni-P(1)	90.0 (6)
I-Ni-P(1)	90.15 (9)	C-Ni-P(2)	90.4 (6)
I′-Ni-P(1)	90.15 (9)	P(1)-Ni-P(2)	179.7 (3)
Distances around P Atoms			
P(1)-C(11)	1.800 (17)	P(2)-C(12)	1.803 (18)
P(1)-C(21)	1.834 (10)	P(2)-C(22)	1.800 (11)
P(1)-C′(21)	1.834 (10)	P(2)-C′(22)	1.800 (11)
Angles around P Atoms			
Ni-P(1)-C(11)	116.7 (5)	Ni-P(2)-C(12)	117.4 (5)
Ni-P(1)-C(21)	113.5 (4)	Ni-P(2)-C(22)	113.4 (4)
Ni-P(1)-C′(21)	113.5 (4)	Ni-P(2)-C′(22)	113.4 (4)
C(11)-P(1)-C(21)	104.1 (5)	C(12)-P(2)-C(22)	103.5 (5)
C(11)-P(1)-C′(21)	104.1 (5)	C(12)-P(2)-C′(22)	103.5 (5)
C(21)-P(1)-C′(21)	103.6 (7)	C(22)-P(2)-C′(22)	104.3 (8)
Ligand-Ligand Distances			
I-I′	4.3248 (15)	I-P(2), I′-P(2)	3.409 (4)
I-C, I′-C	3.845 (19)	C-P(1)	2.816 (22)
I-P(1), I′-P(1)	3.430 (3)	C-P(2)	2.818 (19)
Carbonyl Group Parameters			
C-O	1.137 (20)	Ni-C-O	179.2 (19)

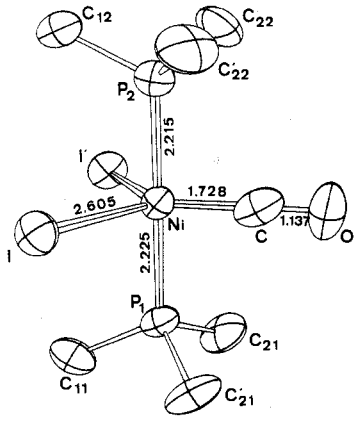

Figure 3. Perspective view of $NiI_2(CO)(PMe_3)_2$.

the nickel atom is trigonal bipyramidal (C_{2v} symmetry) with the two PMe_3 ligands in axial positions and the nickel, the iodine atoms, and the carbon monoxide group in the equatorial plane. The atom-to-equatorial plane distances are as follows: Ni, −0.0005 Å; I′, −0.0007 Å; I, −0.0008 Å; C, 0.0068 Å; O, −0.0048 Å. The only marked distortion of the molecule from the ideal trigonal-bipyramidal geometry lies in the equatorial plane where the I-Ni-C and I′-Ni-C angles of 123.88 (4)° are slightly larger than the ideal value of 120°. Consequently the I-Ni-I′ angle of 112.24 (7)° is smaller than this value. In contrast to what happens in the pentacoordinate TBP $NiBr_2(PMe_3)_3$ and $(NiBr(PMe_3)_4)(BF_4)$ complexes,[11] the P(1)-Ni-P(2) angle of 179.2 (4)° is very close to the value of 180° expected in a regular TBP, thus indicating that the axial-equatorial ligand interaction is minimized. This result may possibly be related to the smaller cone angle of CO (θ = 95°) compared to that of PMe_3 (θ = 118°).[14]

Nickel-phosphorus distances Ni-P(1) = 2.225 (5) Å and Ni-P(2) = 2.215 (5) Å are not significantly different and are well in the range of Ni-P distances observed in pentacoordinate Ni(II)-PR_3 complexes.[11] The Ni-I_{eq} bond lengths of 2.6048 (13) Å compare well with the average Ni-I_{eq} distances of 2.616 (2) Å found in $NiI_2(CO)(fdma)$[9] and the value of 2.661 Å found in $NiI_2(P(OMe)_3)_3$.[20] They are intermediate between the values of 2.80 (2) and 2.49 (2) Å found in TBP $NiI_2(PHPh_2)_3$ where a distortion toward the square pyramid is present.[21] In all these structures, the iodine atoms are located in the equatorial plane of the TBP. On the other hand, they are shorter than the Ni-I_{ax} of 2.71 (1) Å found in the TBP complex $(NiI(tda))^+$ (tda = tris(2-(diphenylphosphino)ethyl)amine),[22] where I is in the axial position. Differences are also found with the Ni-I bond length in square-pyramidal Ni(II) complexes since a distance Ni-I_{ax} of 2.797 Å is found in the square-pyramidal $(NiI(tep)_2)I$[23] (tep = 1,2-bis(diethylphosphino)ethane, where I is in the axial position, and an average value of 2.5405 Å for the basal Ni-I distance in the square-pyramidal $NiI_2(dsp)$[24] (dsp = bis(*o*-(methylthio)phenyl)phenylphosphine). These results are probably related to the different radius of Ni(II) in trigonal-bipyramidal and square-pyramidal geometries and to the σ and π abilities of the ligand in the axial and equatorial sites of the two geometries.[25]

Table X. Ni-C and C-O Bond Lengths in Nickel-Carbonyl Complexes

compd	Ni-C, Å	C-O, Å	ref
$NiI_2(CO)(PMe_3)_2$	1.728 (23)	1.137 (20)	this work
$Ni(CO)_4$	1.82 (3)	1.15 (2)	26
$(c\text{-}C_6H_{11})_3P\cdot C(CH_3)HNi(CO)_3$	1.74 (1)–1.78 (1)	1.14 (2)–1.16 (2)	27
$(C_6H_5)_4P_2(Ni(CO)_3)_2$	1.78 (1)–1.82 (1)	1.10 (1)–1.13 (1)	28
$((C_6H_5)_2PNi(CO)_2)_2$	1.79 (1)	1.13 (1)	29
$(\pi\text{-}C_5H_4As(CH_3)_2Fe)NiI_2(CO)$	1.82 (2)	1.10 (2)	9
$((CNC_2H_4)_3P)_4Ni_4(CO)_6$[a]	1.85 (2)–1.92 (2)	1.19 (2)–1.21 (3)	30
$(\pi\text{-}C_5H_5Ni)_3(CO)_2$[a]	1.93 (2)	1.19 (3)	31
$(\eta\text{-}C_5H_5Ni)_2(\eta\text{-}C_5H_5)Co(CO)_2$[a]	1.93 (1)	1.18 (1)	32

[a] In these compounds CO is a bridging ligand.

The P-C bond lengths (1.800 (17)–1.834 (10) Å), the Ni-P-C angles (113.4 (4)–117.4 (5)°), and the C-P-C angles (103.5 (5)–104.3 (8)°) are well within the range of observed distances and angles for the trimethylphosphine ligand. Due to the presence of the mirror plane, the two axial PMe_3 groups have an eclipsed configuration with the carbon atoms as far as possible from the equatorial atoms. The carbon monoxide group is coordinated in a linear fashion with a Ni-C-O angle of 179.2 (19)°. The most interesting part of this structure is the Ni-C bond length of 1.728 (23) Å, which is to our knowledge the shortest Ni-C distance reported in the literature. Table X gives the other Ni-CO distances found in carbonylnickel complexes. In most of the complexes which possess Ni-C bonds (nickel complexes with olefins, acetylenes, and allyl groups) the Ni-C bond length ranges from 1.90 to 2.10 Å.[2] Comparison with $NiI_2(CO)(fdma)$, which is a TBP Ni(II) complex with the two iodine atoms in equatorial positions but with CO occupying an axial one, shows that the axial Ni-CO bond length of 1.817 (6) Å is significantly longer than the equatorial Ni-CO distance in $NiI_2(CO)(PMe_3)_2$. However, as seen previously, the equatorial Ni-I distances are similar for both complexes. One possibly may rationalize this difference from the strong π-acceptor behavior of CO. When located in the equatorial plane of the TBP with the iodine atoms, it has nearly the exclusive use of the π electrons of the d_{xy} and $d_{x^2-y^2}$ metal orbitals. But when it is located in the axial position of the TBP as in the $NiI_2(CO)(fdma)$ complex, it has to compete with arsenic for the π electrons, resulting in a less effective π back-bonding and in a larger Ni-C distance. However a similar difference in bond lengths has been observed between equatorial and

(20) Vande Griend, L. J.; Clardy, J. C.; Verkade, J. G. *Inorg. Chem.* **1975**, *14*, 710.
(21) Bertrand, J. A.; Plymale, D. L. *Inorg. Chem.* **1966**, *5*, 879.
(22) Dapporto, P.; Sacconi, L. *J. Chem. Soc.* **1970**, 1804.
(23) Alyea, E. C.; Meek, D. W. *Inorg. Chem.* **1972**, *11*, 1029.
(24) Meek, D. W.; Ibers, J. A. *Inorg. Chem.* **1969**, *8*, 1915.
(25) Raymond, K. N.; Corfield, P. W. R.; Ibers, J. A. *Inorg. Chem.* **1968**, *7*, 1362.
(26) Ladell, J.; Post, B.; Fankuchen, I. *Acta Crystallogr.* **1952**, *5*, 795.
(27) Barnett, B. L.; Kruger, C. *J. Cryst. Mol. Struct.* **1972**, *2*, 271.
(28) Mais, R. H. B.; Owston, P. G.; Thompson, D. T.; Wood, A. M. *J. Chem. Soc. A* **1967**, 1744.
(29) Jarvis, J. A. J.; Mais, R. H. B.; Owsten, P. G.; Thompson, D. T. *J. Chem. Soc. A* **1970**, 1867.
(30) Bennet, M. J.; Cotton, F. A.; Winquist, B. H. C. *J. Am. Chem. Soc.* **1967**, *89*, 5366.
(31) Hock, A. A.; Mills, S. *Proc. Int. Conf. Coord. Chem., 6th* **1961**, 640.
(32) Uchtman, V. A.; Dahl, L. F. *J. Am. Chem. Soc.* **1969**, *91*, 3763.

Table XI. Nonbonding Contacts between Axial and Equatorial Ligands in Trigonal-Bipyramidal d^8 Nickel(II) Complexes

compd	geometry	lig_{ax}-lig_{eq}, Å		lig_{eq}-lig_{eq}, Å		ref
$NiI_2(CO)(PMe_3)_2$	cis eq-eq TBP (C_{2v})	P_a-I_e:	3.430 (3) 3.409 (4)	I_e-I_e:	4.3248 (15)	this work
		P_a-C_e:	2.816 (22) 2.818 (19)	I_e-C_e:	3.845 (19)	
$NiI_2(P(OMe)_3)_3$	cis eq-eq TBP (C_{2v})	P_a-I_e:	3.380 (2) 3.448 (2) 3.326 (2) 3.481 (2)	I_e-I_e: I_e-P_e:	4.414 (1) 4.288 (2) 4.249 (2)	20
		P_a-P_e:	3.205 (2) 3.050 (2)			
$[NiBr(PMe_3)_4](BF_4)$	TBP (C_{2v})	P_a-Br_e:	3.180 (4) 3.182 (4)	P_e-P_e: Br_e-P_e:	3.984 (5) 3.964 (5)	11
		P_a-P_e:	3.299 (7) 3.246 (7) 3.301 (6) 3.277 (6)		4.264 (5)	
$[NiBr(P(OMe)_3)_4](BF_4)$	TBP (C_{2v})	P_a-Br_e:	3.192 (2) 3.154 (2)	P_e-P_e: Br_e-P_e:	3.914 (2) 3.900 (2)	34
		P_a-P_e:	3.137 (3) 3.145 (3) 3.198 (2) 3.141 (2)		4.091 (2)	
$NiBr_2(PMe_3)_3$ (2 molecules)	cis eq-eq TBP (C_{2v})	(1) P_a-Br_e:	3.324 3.188 3.284 3.169	(1) Br_e-Br_e: (1) Br_e-P_e:	4.281 3.925 4.236	11
		(1) P_a-P_e:	3.288 3.283			
		(2) P_a-P_e:	3.290 3.224 3.291 3.201	(2) Br_e-Br_e: (2) Br_e-P_e:	4.178 3.946 4.287	
		(2) P_a-P_e:	3.256 3.249			

[a] van der Waals distances: P-I, 4.05 Å; P-Br, 3.95 Å; P-P, 3.8 Å; I-I, 4.30 Å; Br-Br, 4.10 Å.[31]

axial Ni-I distances in TBP Ni(II) complexes: Ni-I_{eq} = 2.6048 (13) Å (this work) and Ni-I_{ax} = 2.71 (1) Å in (NiI(tda))I,[22] thus indicating that the π back-bonding ability of CO is not the only factor responsible for the inequivalent axial and equatorial Ni-CO distances. However, this result is opposite to the reported structure of TBP $(Ni(CN)_5)^{3+}$[33] and $[Ni(P(OR)_3)_5]^{2+}$[34] ($P(OR)_3 = P(OCH)_3(CH_2)_3$) where Ni-$L_{ax}$ distances are smaller than Ni-L_{eq}, as expected for d^8 pentacoordinate TBP complexes. The C-O bond length of 1.137 Å compares well with the value observed in nickel(0) carbonyl complexes (Table VIII) and is also in agreement with the CO distance of 1.30 Å found in gaseous carbon monoxide.

It is tempting to ascribe the differences between the inequivalence of the bond lengths and angles in the TBP Ni(II) complexes to nonbonded intramolecular contacts between the donor atoms coordinated to the metal. Table XI summarizes these contacts for some Ni(II) compounds. It is apparent from these few examples that the intramolecular contacts can be classified in two groups of values: the contacts between axial and equatorial ligands (L_{ax}-Ni-L_{eq} = 90°) correspond to values less than the sum of the van der Waals radii of the relevant atoms while contacts between equatorial ligands (L_{eq}-Ni-L_{eq} = 120°) correspond to values larger than or equal to the sum of the van der Waals radii. An analogous trend is present in similar Co(II) complexes: $CoCl_2(PMe_3)_3$[35] and $CoCl_2(NO)(PMe_2Ph)_2$.[36] From these observations, it can be suggested that the distortions observed for a TBP Ni(II) complex with different monodentate ligands could be considered as occurring inside a cage formed by nonbonding contacts and involving both angles around the nickel atom and the nickel-ligand distances. However, it is certain that the intermolecular packing interactions play a role which has not been investigated.

Thus, while pentacoordinate Ni(II) complexes NiX_2L_3 have only been isolated with sterically nonhindered phosphine (PMe_3, θ = 118°; PMe_2Ph, θ = 122°), pentacoordinate $NiX_2(CO)L_2$ compounds have been synthesized even with PPh_3 (θ = 145°). This is in agreement with the importance of the steric hindrance of the ligands in stabilizing five-coordinate complexes since the CO cone angle is θ = 95°.

In all the complexes, CO and the halogens are located in the equatorial positions of the trigonal bipyramid, in agreement with the already reported conclusions on the relative positions of the ligands in d^8 TBP complexes.[11]

Cationic Complexes $[NiX(CO)(PMe_3)_3](BF_4)$ (X = Cl, Br). Bubbling CO through a dichloromethane/cetane (1/1) or dichloromethane/ethanol (1/1) solution of $[NiBr(PMe_3)_4](BF_4)$ shows, contrary to the molecular complexes, the presence successively of (i) the cationic Ni(II) compound $[NiBr(CO)(PMe_3)_3](BF_4)$ (ν_{CO} = 2030 cm^{-1}), (ii) the Ni(0) species $Ni(CO)_2(PMe_3)_2$ (ν_{CO} = 1920 and 1990 cm^{-1}), and (iii) the Ni(0) species $Ni(CO)_3(PMe_3)$ (ν_{CO} = 1990 and 2060 cm^{-1}).[30] The reduction is faster when ethanol is present.

The cationic Ni(II) complexes $[NiX(CO)(PMe_3)_3](BF_4)$ have been isolated by following reaction 3. They are obtained as orange needles,

$$[NiX(PMe_3)_4](BF_4) + CO \xrightarrow[1\ atm]{20\ °C} [NiX(CO)(PMe_3)_3](BF_4) + PMe_3\uparrow \quad (3)$$

evolving CO easily in giving the pink tetracoordinate $[NiX(PMe_3)_3](BF_4)$ compound, characterized by its chemical analysis. Only $[NiBr(CO)(PMe_3)_3](BF_4)$ is stable enough to be studied. $[NiI(CO)(PMe_3)_3](BF_4)$ has not been isolated. When CO reacts with the cationic $[NiI(PMe_3)_4](BF_4)$ species, only the molecular more stable $NiI_2(CO)(PMe_3)_2$ precipitates, due to the presence of an equilibrium in dichloromethane solutions between the two species.[11]

$[NiBr(CO)(PMe_3)_3](BF_4)$ is pentacoordinated as shown by its chemical analysis. Its insolubility in nonpolar solvents, such as benzene, prevents its molecular weight determination. Its solid-state IR spectrum shows only one ν_{CO} at 2030 cm^{-1}, indicating only one isomer. The higher value, compared to the molecular $NiBr_2(CO)(PMe_3)_2$

(33) Raymond, K. N.; Corfield, P. W. N.; Ibers, J. A. *Inorg. Chem.* **1972**, *11*, 828.
(34) Milbrath, O. S.; Springer, J. P.; Clardy, J. C.; Verkade, J. G. *Inorg. Chem.* **1975**, *14*, 2665.
(35) Alnaji, O. Thesis, Toulouse, 1978.
(36) Rossi, A. R.; Hoffmann, R. *Inorg. Chem.* **1975**, *14*, 365.
(37) Sharpley, J. R.; Osborn, J. A. *Acc. Chem. Res.* **1973**, *6*, 305.
(38) Churchill, M. R.; Lin, K. G. *J. Am. Chem. Soc.* **1974**, *96*, 76.
(39) Goldfield, S. A.; Raymond, K. N. *Inorg. Chem.* **1974**, *13*, 770.

(2010 cm^{-1}) is in agreement with the presence of a positive charge on Ni(II), decreasing the Ni–CO back-bonding. The electronic spectral data (Table VII) show, in the low-energy range, a three-band system which is better resolved at 190 K. This spectral pattern is similar to the one previously observed for the molecular $NiBr_2(CO)(PMe_3)_2$ complex and indicates the presence of a TBP geometry of low symmetry. The ^{31}P NMR data show at about 163 K (in CD_2Cl_2/CF_2ClH, 1:1 ratio) the presence of a ill-resolved doublet at 17 ppm and triplet at −26.6 ppm (62.5% H_3PO_4 as reference). At this temperature, $[NiCl(CO)(PMe_3)_4](BF_4)$ is still stereononrigid since only a singlet at 6.14 ppm is observed. Comparison with the ^{31}P NMR data obtained on the NiX_2–PMe_3 TBP complexes, where it has been possible to differentiate axial and equatorial PMe_3 by the corresponding ^{31}P chemical shift, indicates for $[NiBr(CO)(PMe_3)_3](BF_4)$ (X = Cl, Br) a trigonal-bipyramidal geometry with X and CO in equatorial position as the more probable structure:

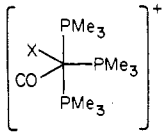

Discussion

Contrary to the literature results,[6,7] no reduction of molecular Ni(II) complexes $NiX_2(PR_3)_n$ (n = 2, 3; X = halide; PR_3 = PMe_3, PEt_3, PMe_2Ph, $PMePh_2$, PPh_3) is observed, in normal conditions of temperature and pressure, when CO is bubbled through dichloromethane or benzene solutions of the complexes. However, when PR_3 = PPh_3 and the solvent is ethanol, fast reduction of Ni(II) to Ni(0) is observed. Such an easier reductive capability of (triphenylphosphine)nickel(II) complexes, compared to trialkylphosphine ones, has been observed in the synthesis of nickel(I) phosphine complexes[40] and nitrosylnickel compounds.[41]

Thus, 1 mol of CO reacts with 1 mol of nickel(II) phosphine complex, either four-coordinate or five-coordinate species. It is apparent from the color change of the solution that, when the pentacoordinate complexes are used as starting material, the first step is the loss of a phosphine ligand, in agreement with the dissociative equilibrium (4). This is confirmed since

$$NiX_2(PMe_3)_3 \rightleftharpoons NiX_2(PMe_3)_2 + PMe_3 \qquad (4)$$

either adding PMe_3 in excess or lowering the temperature, i.e., stabilizing the pentacoordinate species by displacing reaction 4 to the left side, prevents any CO fixation.

Then, 1 mol of CO reacts with 1 mol of the tetracoordinate Ni(II) complex, either the low-spin square-planar species when PR_3 = PMe_3, PEt_3, or PMe_2Ph or the tetrahedral ones when PR_3 = $PMePh_2$ or PPh_3, to give the five-coordinate carbonyl species according to reaction 5. When more CO is added,

$$NiX_2(PR_3)_2 + CO \rightleftharpoons NiX_2(CO)(PR_3)_2 \qquad (5)$$

nothing occurs. No complex, including two CO ligands, can be characterized as was the situation when $P(OMe)_3$ was substituted for PMe_3 in the $NiX_2(PMe_3)_3$ compounds. There, it was possible to characterize the two species $NiX_2(PMe_3)_2(P(OMe)_3)$ and $[NiX(PMe_3)_2(P(OMe)_3)_2]X$ as TBP complexes with stereochemistries I and II (X = halide).[42]

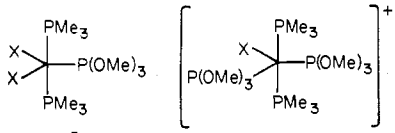

I II

However the cationic species $[NiX(PMe_3)_4](BF_4)$ behaves differently toward CO. Reduction of Ni(II) to Ni(0) occurs when an excess of CO is bubbled through the solution. The reduction is faster when ethanol is used as solvent. The mechanism of this reduction has not yet been determined. Reduction by a trace of water in the solvent has been invoked to explain the reduction of analogous cationic Co(II) complexes by CO.[43] Another pathway, which may be envisaged, is through substitution of a second PMe_3 ligand by CO in excess, following reactions 6 and 7. The dicarbonyl complex, unstable, decomposes giving rise to the nickel(0) species (eq 7). A third possibility in methanol or ethanol is a pathway through a Ni–(COOR) complex formation, as has been observed for Pt(II) complexes[5] and for $[Ni(C_6H_5)(CO)(PR_3)_2]^+$[10] since a color change is observed when MeOH or EtOH is added to a dichloromethane solution of $(NiBr(CO)(PMe_3)_3)(BF_4)$. But we have not succeeded yet in isolating a definite complex.

$$[NiBr(CO)(PMe_3)_3](BF_4) + CO \rightarrow [NiBr(CO)_2(PMe_3)_2](BF_4) + PMe_3 \qquad (6)$$

$$[NiBr(CO)_2(PMe_3)_2](BF_4) \rightarrow Ni(CO)_2(PMe_3)_2 + BrBF_4 \qquad (7)$$

In conclusion, CO reacts on nickel(II) phosphine complexes $NiX_2(PR_3)_n$ (n = 2, 3; X = halide), giving rise to five-coordinate TBP complexes with CO in the equatorial position. The nature of the Ni(II) complex, either low-spin or high-spin tetracoordinate or pentacoordinate species, does not play a particular role. The stabilization of these pentacoordinate carbonylnickel(II) complexes can be related to (1) the presence of the two halide ligands sharing with CO the equatorial positions of the TBP and (2) the fact that no insertion reaction of CO in a metal halide bond has been reported. When the CO insertion reaction may occur, for example, in the formation of the acylnickel(II) complex $NiX(COCH_3)(PMe_3)_2$[3] or in the synthesis of $Ni(NO)(NO_2)(PR_3)_2$ by reaction of CO on $Ni(NO_2)_2(PR_3)_2$,[45,46] pentacoordinate nickel(II) carbonyl complexes can be envisaged as the first-step intermediate (reactions 8 and 9).

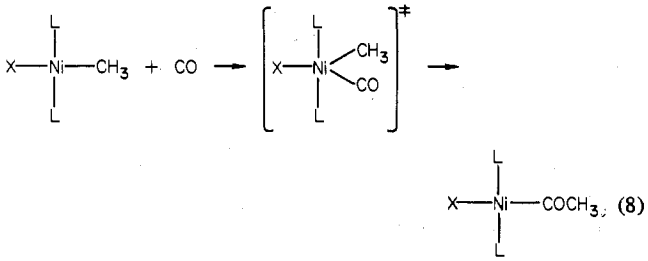

(8)

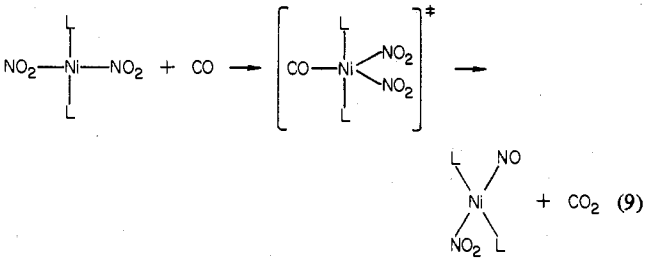

(9)

Registry No. $NiCl_2(CO)(PMe_3)_2$, 73697-46-8; $NiBr_2(CO)(PMe_3)_2$, 70252-74-3; $NiI_2(CO)(PMe_3)_2$, 35872-05-0; $NiBr_2(CO)(PMe_2Ph)_2$, 73687-91-9; $NiI_2(CO)(PMe_2Ph)_2$, 73687-92-0; $NiBr_2(CO)(PMePh_2)_2$,

(40) Caballero, F.; Gomez, M.; Royo, P. *Transition Met. Chem. (N.Y.)* **1977**, *2*, 130.
(41) Feltham, R. D. *Inorg. Chem.* **1964**, *3*, 116.
(42) Meier, P.; Merbach, A.; Dartiguenave, M.; Dartiguenave, Y. *Inorg. Chim. Acta* **1980**, *39*, 19.
(43) Albertin, C.; Bordignon, E.; Orio, A. A.; Rizzardi, G. *Inorg. Chem.* **1975**, *14*, 944.
(44) Calderazzo, F. *Angew. Chem., Int. Ed. Engl.* **1977**, *16*, 299.
(45) Bhaduri, S.; Johnson, B. F.; Matheson, T. W. *J. Chem. Soc., Dalton Trans.* **1977**, 561.
(46) Feltham, R. D.; Kriege, J. *J. Am. Chem. Soc.* **1979**, *101*, 5064.

73687-93-1; $NiI_2(CO)(PMePh_2)_2$, 73687-94-2; $NiBr_2(CO)(PPh_3)_2$, 73687-95-3; $NiI_2(CO)(PPh_3)_2$, 73687-96-4; $NiBr_2(CO)(PEt_3)_2$, 73687-97-5; $NiI_2(CO)(PEt_3)_2$, 73687-98-6; $[NiCl(CO)(PMe_3)_3](BF_4)$, 70252-79-8; $[NiBr(CO)(PMe_3)_3](BF_4)$, 70252-77-6; $NiI_2(PMe_3)_3$, 53188-34-4; $[NiCl(PMe_3)_4](BF_4)$, 60919-88-2; $[NiBr(PMe_3)_4](BF_4)$, 60919-89-3.

Supplementary Material Available: Table III, a listing of observed and calculated structure amplitudes (3 pages). Ordering information is given on any current masthead page.

Contribution from the Department of Chemistry,
The University of Texas at Arlington, Arlington, Texas 76019

Base-Catalyzed Bimodal Cleavage of Ethylaquocobaloxime[1,2]

KENNETH L. BROWN* and RITA K. HESSLEY

Received January 22, 1980

The base-catalyzed decomposition of ethylaquocobaloxime has been studied by GLC, mass spectrometry, and manometric techniques at 50.0 ± 0.1 °C in aqueous solution and in D_2O. Under all conditions, a mixture of ethane and ethylene is obtained, and no photolabile organocobalt complex is formed. In D_2O the alkane product is monodeuterioethane of high isotopic purity, but little or no deuterium is incorporated into the alkene product. Unreacted starting material recovered from partial decomposition in alkaline D_2O was found to have very little deuterium incorporated into its alkyl ligand. From the dependence of the product ratio on base concentration, the observed rate constant for decomposition in 1.0 M base and the spectrophotometrically determined dissociation constants for the hydroxo (and deuterioxo) species the specific second-order rate constants for the alkene-forming reaction ($(1.06 \pm 0.06) \times 10^{-6}$ M^{-1} s^{-1} and $(3.21 \pm 0.12) \times 10^{-6}$ M^{-1} s^{-1} for the anionic hydroxo species in H_2O and D_2O, respectively, and $(5.36 \pm 0.43) \times 10^{-7}$ M^{-1} s^{-1} and $(2.20 \pm 0.15) \times 10^{-6}$ M^{-1} s^{-1} for the neutral aquo species in H_2O and D_2O, respectively) and the alkane-forming reaction ($(6.05 \pm 0.35) \times 10^{-6}$ M^{-1} s^{-1} and $(5.87 \pm 0.73) \times 10^{-6}$ M^{-1} s^{-1} for the hydroxo species in H_2O and D_2O, respectively, and zero for the aquo species in both solvents) have been determined. The large inverse solvent deuterium isotope effects for the alkene-forming reaction are discussed in terms of a likely E2 mechanism. The mechanism of the alkane-forming reaction cannot be determined from the present data but is discussed in light of the recent results for methane formation from methylaquocobaloxime in aqueous base. It is concluded that the mechanism of the alkane-forming reaction may not be the same for the two organocobaloximes.

Introduction

In recent reports[3,4] one of us described quantitative experiments on the heterolysis of methylaquocobaloxime in aqueous base at 50 °C, evidently an example of mode III cleavage[4] of a simple, unactivated organocobalt complex. This reaction leads to the formation of methane in about 70% yield and a base-stable but photolabile methylcobalt side product in about 30% yield. Although Schrauzer[5] has stated that higher alkylcobaloximes decompose in aqueous base to form olefins and cobaloxime(I) (i.e., mode I cleavage[4]), our preliminary GLC analysis of the products of the decomposition of ethylaquocobaloxime in aqueous base showed that mixtures of ethane and ethylene were always obtained. As this reaction seemed to provide an opportunity to simultaneously study mode I and mode III cleavages as well as to extend our earlier work on the base-catalyzed mode III cleavage of simple organocobalt complexes, we undertook a quantitative study of the base-catalyzed decomposition of ethylaquocobaloxime. The present report describes the results of our study including the kinetics of ethylaquocobaloxime decomposition and the dependence of both cleavage modes on base concentration in both water and D_2O at 50 °C.

Experimental Section

Materials. Cobaltous chloride, methyl sulfide, sodium borohydride, sodium and potassium hydroxides, potassium chloride, potassium nitrate, methanol, dimethylglyoxime, ethyl bromide, and pyridine were obtained in the highest purity commercially available and used without further purification. Deuterium oxide (99.8 atom % D) and sodium deuterioxide (40% solution in D_2O, 99+ atom % D) were from Aldrich. Glass-distilled deionized water was used throughout.

$CH_3CH_2Co(D_2H_2)OH_2$ was synthesized and characterized by the procedures previously described.[6]

$CH_3CH_2Co(D_2H_2)py$ was obtained from the aquo complex as follows. A 250-mg sample of $CH_3CH_2Co(D_2H_2)OH_2$ was dissolved in about 25 mL of methanol with stirring. Upon addition of 1 mL of pyridine, the solution changed from orange to yellow immediately. After an additional 10 min of stirring, 25 mL of water was added, and the volume was reduced to about 25 mL on a rotary evaporator. After cooling of the solution in ice, the yellow solid was collected by vacuum filtration and dried over P_2O_5 under vacuum (yield 64%).

Unreacted $CH_3CH_2Co(D_2H_2)OH_2$ from partial decomposition in aqueous base was recovered as the pyridine complex in the following manner. A 0.5-g sample of $CH_3CH_2Co(D_2H_2)OH_2$ was dissolved in 25 mL of 1.0 N aqueous KOH (or 1.0 N NaOD/D_2O) which had been purged with argon for 30 min. Under continuous argon purge, the reaction mixture was heated to 50 °C in the dark for 24 h (i.e., approximately 1 half-time). The reaction mixture was then cooled in ice and neutralized with concentrated HCl (or 20% DCl in D_2O). Addition of 1 mL of pyridine caused immediate formation of a yellow precipitate which was collected by vacuum filtration and dried over P_2O_5 under vacuum.

Methods. Ethylcobaloximes were handled in dim light, and solutions were covered with aluminum foil whenever possible. Ionic strength was maintained at 1.0 M with KCl or KNO_3.

The apparent dissociation constants $K_D^{OH^-}$, for hydroxide ion from $CH_3CH_2Co(D_2H_2)OH^-$, and $K_D^{OD^-}$, for deuterioxide ion from $CH_3CH_2Co(D_2H_2)OD^-$ (eq 1 and 2), were determined spectrophotometrically at 50.0 ± 0.1 °C with an ionic strength of 1.0 M (KCl)

$$CH_3CH_2Co(D_2H_2)OH^- \underset{\pm OH^-}{\overset{K_D^{OH^-}}{\rightleftharpoons}} CH_3CH_2Co(D_2H_2)OH_2 + OH^- \quad (1)$$

$$K_D^{OH^-} = [CH_3CH_2Co(D_2H_2)OH_2][OH^-]/[CH_3CH_2Co(D_2H_2)OH^-] \quad (2)$$

(1) This project was supported by the National Institutes of Health, the U.S. Public Health Service (Grant GM23215), and the Robert A. Welch Foundation, Houston, Texas (Grant Y-749).
(2) Abbreviations: $RCo(D_2H_2)L$ = alkyl(ligand)bis(dimethylglyoximato)cobalt(III) = alkyl(ligand)cobaloxime; py = pyridine.
(3) Brown, K. L. *Inorg. Chim. Acta* **1978**, *31*, L401–L403.
(4) Brown, K. L. *J. Am. Chem. Soc.* **1979**, *101*, 6600–6606.
(5) See footnote 16 in: Schrauzer, G. N.; Weber, J. H.; Beckham, T. M. *J. Am. Chem. Soc.* **1970**, *92*, 7078–7086.
(6) Brown, K. L.; Lyles, D.; Pencovici, M.; Kallen, R. G. *J. Am. Chem. Soc.* **1975**, *97*, 7338–7346.

0020-1669/80/1319-2410$01.00/0